Redox Biology 83 (2025) 103637

Contents lists available at ScienceDirect

Redox Biology

journal homepage: www.elsevier.com/locate/redox

OXPHOS inhibition overcomes chemoresistance in triple negative breast cancer

Cemile Uslu [1], Eda Kapan [1], Alex Lyakhovich [*]

Sabanci University, Molecular Biology, Genetics and Bioengineering, Faculty of Engineering and Natural Sciences, Turkey

ARTICLE INFO

Keywords:
Oxidative phosphorylation
Cancer resistance
Triple negative breast tumors
Mitochondria
Autophagy
Antimicrobials

ABSTRACT

The hypothesis of a significant shift from oxidative phosphorylation (OXPHOS) to glycolysis in a number of solid tumors has been dominant for many years. Recently, however, evidence has begun to accumulate that OXPHOS is the major mode of energy production in many neoplasias, especially those that have undergone chemo- or radiotherapy, and especially in chemoresistant malignancies. In the present work, we demonstrated that chemoresistant triple-negative breast cancer cells prefer to obtain energy via OXPHOS to a greater extent than cells sensitive to chemotherapeutic agents, and therefore the former can be affected by some OXPHOS inhibitors. From a drug library containing several dozen antimicrobials, we selected those that inhibit OXPHOS in resistant TNBC cells and lead to mitochondrial dysfunction. We have also identified several pathways by which inhibition of growth suppression of chemoresistant cells occurs, including increased oxidative stress and mitophagy. Experiments in mice showed that selected OXPHOS inhibitors preferentially suppress tumor growth from chemoresistant but not from chemosensitive cells. The results of the present study suggest combinatorial therapy of such inhibitors and conventional anticancer drugs on resistant forms of tumors, if the latter show enhanced OXPHOS.

1. Introduction

Despite undoubted progress in the treatment of breast cancer (BC), which ranks first among the causes of cancer-related mortality in women [1], the 5-year survival rate of patients remains relatively low, and for some forms of BC, especially distant triple negative breast cancer (TNBC) is only 12 % [2]. The standard treatment modalities for BC patients are surgical destruction followed by radio- and/or chemotherapy. TNBC, one of the most common histologic subtypes of BC, initially responds well to platinum- or phosphamide-based chemotherapy, but over time patients relapse and develop chemoresistance [3]. The development of chemoresistance is a major obstacle to improving survival of BC patients, as it leads to metastasis and eventually death of patients [4].

In most solid tumors, including TNBC, a set of different and not fully understood mechanisms is responsible for the development of chemoresistance and disease recurrence [5]. In particular, the hypothesis put forward by Otto Warburg about the transition of cancer cells to the glycolytic pathway of energy production even in the presence of sufficient oxygen, dominated for many years [6,7]. Later, after detailed elucidation of mitochondrial functions, it was modified into the hypothesis of metabolic switching implying the transition of cell bioenergetics from oxidative phosphorylation (OXPHOS) to glycolysis [8]. This hypothesis also raised certain questions about higher energy demand of proliferating cancer cells, but was partially explained by the faster kinetics of glycolysis in relation to OXPHOS [9]. Recently, however, numerous data have begun to accumulate that OXPHOS is the major mode of energy production in many malignant tumors, particularly those exposed to chemo- or radiotherapy [10]. For example, there are many studies showing overexpression of OXPHOS genes and proteins in ovarian [11,12], breast [13], colon [14–16] lung [17], pancreatic cancers [18,19] as well as in acute myeloid leukemia (AML) [20,21], lymphoma [22,23] and melanoma [24,25].

For this reason, mitochondrial OXPHOS suppression may serve as an alternative or adjunct to conventional anticancer therapy in cases where standard treatment is not feasible [26,27]. However, since OXPHOS is a key process that ensures the vital functions of the living organism, the selection of suitable low-toxicity inhibitors is a non-trivial task. To this end, antimicrobials have been proposed because they can target not only

* Corresponding author. Molecular Biology, Genetics and Bioengineering Program, Faculty of Engineering and Natural Sciences, FENS 1043, Sabancı Üniversitesi, Üniversite Caddesi No: 27, Orta Mahalle, Tuzla, İstanbul, 34956, Turkey.
E-mail addresses: alex.lyakhovich@sabanciuniv.edu, lyakhovich@gmail.com (A. Lyakhovich).
[1] Equal contribution.

https://doi.org/10.1016/j.redox.2025.103637
Received 2 April 2025; Accepted 13 April 2025
Available online 15 April 2025

Abbreviations

ΔΨ M	Mitochondrial membrane potential
OCR	consumption rate
ATP5MF	ATP synthase membrane subunit F
COX5A	Cytochrome C oxidase subunit 5A
COX6A	Cytochrome C oxidase subunit 6A
CSC	Cancer stem cells
LDHA	Lactate dehydrogenase A
mtDNA	Mitochondrial DNA
MMPs	matrix metalloproteases
NAD +	Nicotinamide adenine dinucleotide
NAMPT	Nicotinamide phosphoribosyltransferase
NDUFA11	NADH ubiquinone oxidoreductase subunit 11
NDUFS6:	NADH ubiquinone oxidoreductase subunit 6
BC	Breast cancer
OXPHOS	Oxidative phosphorylation
PDK1	Pyruvate dehydrogenase kinase
PKM2	Pyruvate kinase isozyme M2
RT-qPCR	Reverse transcriptase-quantitative polymerase chain reaction
ROS	Reactive oxygen species
TIMM17A	Translocase of the inner mitochondrial membrane
UQCR10	Ubiquinol-cytochrome C reductase subunit X

Gram-negative bacteria but also double-walled mitochondria, a relic of alphaproteobacteria [28,29]. More specifically, some antibiotics are able to affect mitochondrial biogenesis in patients with early-stage breast cancer to reduce the population of cancer stem cells (CSC) responsible for the hypermetabolic phenotype of tumor cells [30,31].

In the current work, we have shown *in vitro* and in vivo how some antimicrobials inhibit the growth of OXPHOS-dependent cancer cells. Using TNBC models, we have demonstrated that chemoresistant cancer cells prefer to obtain energy through OXPHOS more than chemosensitive cancer cells and therefore the former can be targeted by some OXPHOS inhibitors. From a drug library containing several hundred antimicrobials we selected those that inhibit OXPHOS in resistant TNBC cells and lead to mitochondrial dysfunction (MDF). Oxidative stress was found to be a major driver of antimicrobial-induced MDF, leading to activation of mitophagy, as well as inhibiting metalloproteinase activity and reducing the metastatic potential of chemoresistant TNBC cells. Experiments on mice have shown that selected OXPHOS inhibitors preferentially suppress tumor growth from chemoresistant but not from chemosensitive cells. This gives grounds to propose a combinatorial effect of such inhibitors and conventional anticancer drugs on resistant forms of tumors, if the latter demonstrate an enhanced OXPHOS.

2. Methods

2.1. Cell lines and treatment

MDA-MB-468, MDA-MB-231, MCF7, human dermal fibroblasts (DF) commercial cell lines were purchased from ATCC and authenticated in Ana Janec's lab (UPF, Barcelona). Cells were cultured in Dulbecco's modified Eagle's medium supplemented with 10 % FBS, 1 % Sodium Pyruvate and 1 % L -glutamine. Chemoresistant cell lines were established with continuous treatment for 6 months with escalating doses of anticancer therapeutic agents such as cyclophosphamide (starting from IC20 of 4.7uM) and cisplatin (starting from IC20 of 8.3uM). Experiments related to measurement of respiration, ATP levels and activities of mitochondrial complexes were performed in the media containing no antibiotics.

2.2. JC-1 staining to determine the mitochondrial membrane potential (ΔΨm)

JC-1 staining was performed according to the manufacturer's protocol (Thermo Fisher, #T3168). Cells (1×10^6) cultured for 24 h and treated with IC50 doses of chemotherapeutic agents for 3 days were harvested, washed with PBS and resuspended in 1 ml PBS. JC-1 stock solution was prepared in DMSO at a concentration of 5 mg/mL. JC-1 dye was then added to the resuspended cells at a final concentration of 2 μg/mL followed by incubation at 37 °C, 5 % CO_2 for 30 min. After incubation, the cells were washed with PBS, plated into 96 well plates (1×10^4 per well) in 100 μl transparent media and analyzed spectrofluorimetrically. The average red and green intensity values in each biological replica were determined and the red and green intensity ratio for each was calculated. The average value for all 3 biological replicates was plotted.

2.3. Analysis of mitochondrial mass content

Mitochondrial mass content was determined as previously described [32]. Briefly, 1×10^6 cells were seeded and incubated at 37 °C and 5 % CO_2 for approximately 24 h after which cells were stained with mitoGreen (1 μM final), washed with PBS, resuspended in 100 μl PBS, and analyzed spectrofluorimetrically by determining the mean green intensity value in each well relative to the unstained control. The ratio of signal intensities for each sample was then calculated and the mean value for all 3 biological replicates was plotted.

2.4. Chemoresistant tumor samples and preparation

Triple negative breast tumor patient samples and minimal data annotation included in this study were provided by the Tumor Bank of Vall d'Hebron University Hospital Biobank (PT13/0010/), integrated in the Xarxa de Bancs de Tumors de Catalunya, and were processed following standard operating procedures with the appropriate approval of the Ethical and Scientific Committees. From the cohort of tumor samples from patients of similar age, eight were processed as they showed uniform distribution of cell mass with minimal fat content. Samples were stored on dry ice, homogenized with a pestle and lysed with RIPA buffer (0.5 M Tris-HCl, pH 7.4, 1.5 M NaCl, 2.5 % deoxycholic acid, 10 % NP-40, 10 mM EDTA, 2 % SDS). After sonication on ice (30 bursts for 20 s each) and centrifugation at 4C at 15000 RPM, supernatants were collected. Samples were normalized to total VDAC protein concentrations by Western blotting procedure.

2.5. Intracellular and mitochondrial ROS

Both intracellular and mitochondrial ROS measurements were performed based on our early established procedures [33]. Measurements of intracellular ROS were based on the ability of cells to oxidize fluorogenic dye 2,7-dichlorofluorescein (H2DCF-DA) to their corresponding fluorescent analogues, that allowed ROS determination in living cells. Mitochondrial ROS was detected by measuring mitochondrial super oxide with MitoSOX red reagent according to the manufacturer's protocol (Invitrogen, Thermo Scientific, M36008). determining the mean green intensity value in each well relative to the unstained control. The signal intensities for each sample were calculated, subtracted from the control of autofluorescence samples, and the mean value for 3–5 biological replicates followed by plotting on the graph.

2.6. Measurement of ATP level

ATP level was measured using ATPlite kit as described in the manufacturer's manual (PerkinElmer, Spain, 6016943). A solution of 10,000 cells in 100 ml media/well was plated in triplicates in a black 96-well plate with clear bottom. 50ul of reagent was added to each well and the plate was mixed for 5 min on an orbital shaker to induce cell lyses followed by incubation in the dark for 10 min to stabilize luminescence. The ATP content was then measured with Biotek's Synergy Mx luminometer.

2.7. Oxygen consumption rate (OCR) measurement with Hansatech oxygraphy

The Hansatech oxygraphy plus system was used for the oxygen uptake measurement which involves the monitoring of oxygen levels in a closed chamber over time to assess the mitochondrial or cellular respiration (Hansatech Instruments Ltd., UK, 2023). This system uses a Clark-type oxygen electrode which detects the changes in the dissolved oxygen levels as the sample consumes oxygen over time. For the calibration, the oxygraph was blanked using the KCl electrolyte to establish baseline oxygen levels. Then 1 mL of the nauplii resuspended in the saline water was placed in the oxygraph chamber to measure the OCR. The procedure was repeated several times ($n > 3$).

2.8. Mitochondrial profiling with Seahorse XFe-24 analyzer

To measure OCR, the Seahorse apparatus (Agilent Technologies Spain, S.L.) was used. In short, 50,000 cells per well were seeded in triplicates or quadruplicates into XFe 24-well plates and treated with antibiotics. After 72 h of treatment, cells were washed with PBS and prewarmed XF assay media (Agilent, 102353–100), supplemented with 5,5 m M glucose, 2 m M pyruvate and 2 mM L -glutamine was added to each well. Cells were then maintained at 37 °C in a non-CO2 incubator for 1 h. Cell Mito Stress Test kit was used to measure mitochondrial parameters by XF24 Analyzer. Measurements were normalized with a posterior BCA assay.

2.9. Mitochondrial complex activity measurement

The activity of mitochondrial OXPHOS Complex I (NADH dehydrogenase) and Complex III were measured with kits (ab109721 and ab109905, respectively, both from Abcam, UK) according to the manufacturer's manual. The specific enzymes were immunocaptured within the wells of the 96-well microplate. Complex I activity was determined following the oxidation of NADH to NAD and the simultaneous reduction of a dye which leads to increased absorbance at OD 450 nm. The activity of complex III was measured using the following formula provided in the Manufacturers manual: CIII activity Rate/sample Rate background (row A/H). Complex III activity is proportional to the increase in absorbance at OD 550 nm examined in the linear phase of the reaction progress curves. The mitochondrial complex II (succinate-coenzyme Q reductase) activity was measured using the mitochondrial complex II colorimetric assay kit (E-BC-K150-M, from Elabscience, USA) according to the manufacturer's manual. Coenzyme Q, a key product of mitochondrial complex II, facilitated the reduction of 2,6-dichloroindoxol, which exhibits a distinct absorption peak at 600 nm. Consequently, the activity of mitochondrial complex II was determined by monitoring the alteration in OD value at 600 nm. Measurements were normalized with a simultaneously performed BCA assay.

2.10. Western blotting and sample preparation

Analyses was performed essentially as described in Kumari et al. [34]. Samples were equilibrated for protein using a BCA assay and lysates were separated on 75 % or 4–20 % acrylamide gels, blotted on nitrocellulose membranes and incubated overnight with the appropriate primary antibodies: b-actin, p62 (#8025), LC3ab (#3868), PINK1 (D8G3 #6946), Parkin (#2132), VDAC (#4866) (all from Cell Signaling, Spain) followed by detection with corresponding HRP-conjugated secondary antibodies (Sigma).

2.11. Cell adhesion assay

Cell adhesion assay was performed as described previously [35]. Shortly, cells were treated with corresponding OXPHOS inhibitors for 24 h, washed in PBS, counted and an equal number of cells were plated in 24-well plates allowing them to attach to the surface. After 30 min of agitation on a shaker, each plate was washed with PBS until no floating cells remained and then cross-linked with 4 % paraformaldehyde for 10 min, replaced with the fresh PBS, stained with crystal violet for 5 min, washed 3 times with PBS and dried. Stained cells were dissolved in 1 % SDS and DMSO/ethanol mixture (50/50 v/v) and absorbance was measured at 570 nm with an ELISA plate reader. The experiment was repeated three times, and for each dish, four wells were scored.

2.12. Migration (wound healing) assay

The assay was performed essentially as described earlier [36]. Briefly, cells were grown to confluence on a u-slide (ibidi GmbH, Germany), and a "wounding" line appeared after removing plastic inserts from the cell monolayer. The width of the wound was measured under a microscope after 0 and 28 h to assess the migration ability of the cells. Results were analyzed with the Student *t*-test.

2.13. Tumorsphere formation

To obtain cancer stem-like cells (tumospheres), we followed previously published protocol [35]. Shortly, a single suspension of corresponding TNBC cells was prepared using enzymatic disaggregation (1 × Trypsin-EDTA, Gibco, 25300062), and the cells were plated at a density of 10.000–12.000 cells per ml in a Cancer Stem Cell medium (C-28070, PromoCell, Heidelberg, Germany) in poly-2-hydroxyethyl methacrylate (Poly-HEMA, Santa Cruz Biotechnology, Dallas, TX, USA, sc-253284)-coated plates. Cells of the first generation (G1) were collected 6 days after seeding. For experiments, third generation of tumorspheres was treated with antimicrobial compounds or DMSO (control), followed by the abovementioned procedure of tumorsphere formation. The relative numbers of tumourspheres per 4 squares were counted manually. The experiments were performed independently at least 2 times, with several replicates.

2.14. Colony formation assays

The assay was performed essentially as described previously [37]. Shortly, cells were suspended in colorless DMEM media containing 0,2 % agarose in the presence or absence of OXPHOS inhibitors and layered in triplicates over a solid base of 0,6 % agarose in 6 well plates. Cells were incubated at 37 °C for 2 weeks and the average number of colonies per well was counted.

2.15. Transmission electron microscopy (TEM)

TEM was performed essentially as described earlier [32]. Shortly, cells were washed with PBS and fixed in 2 % paraformaldehyde in PBS for 60 min at RT. The cells were embedded in LR White medium (Polysciences Inc., London, UK) and the labeling of the ultrathin sections was performed on grids. The specimens were contrasted with 2.5 % uranyl acetate (Lachema-Pliva, Brno, Czech Republic) for 20 min and with Reynolds' solution (Sigma) for 8 min at RT. The specimens were then observed using a Morgagni 268 (D) transmission electron microscope (FEI Company, Hillsboro, OR, USA). The images were captured by a

MegaView III CCD camera (Soft Imaging System).

2.16. Artemia salina maintenance for in vivo drug testing

For toxicity and mtROS assay, maintenance and hatching of *A. salina* was designed as recently described [38] Treatment with OXPHOS inhibitors was done on the day 3 after cyst hatching. Shortly, the dry cysts (1g of Ocean Nutrition, batch number: 0N13280) were incubated in a well-aerated (air pump) 1.5 L aquarium with a thermostat submerged into artificial salty water (17 g/L of Tropic Marin Pro Reef Sea Salt). The aquarium was placed on magnetic stirrer with 300 rpm and the thermostat was set at 28 °C for 14 h light/10 h dark photoperiod. On the 3rd day, the stirrer was stopped in order for the eggs to settle down for 15 min and fresh nauplii were collected by positive phototaxis using light to direct them to a specific region followed by distributed across 6 × 50 ml burettes covered with aluminum foil leaving the bottom exposed to light, and left for 2 h. Approximately 1 ml from every burette was poured into a single 50 ml falcon tube to allow for the manual counting of nauplii under a light microscope (average range between 800 and 1000 species). For mitochondrial ROS levels, the same procedure was performed in Vi-Cell viability analyzer after staining with mitochondrial superoxide indicator MitoSOX™ red followed by fluorescence measurement on fluorescence plate reader at the excitation/emission wavelengths 510/580 nm. Viability was determined manually.

2.17. Xenograft studies

All animal experiments were carried out in accordance with the U.K. Animals (Scientific Procedures) Act, 1986 and associated guidelines, EU Directive 2010/63/EU for animal experiments, or the National Research Council's Guide for the Care and Use of Laboratory Animals. Ethical committee approval has been obtained before the experiments (CEEA Vall d'Hebron Institut de Recerca). 8-week female NMRI-nu mice were purchased from Janvier Labs (France) and housed in a pathogen-free environment. Power analysis using data from the pilot experiment showed that 4 mice per group would provide 80 % power to detect differences in the % of resistant cells in the drug treated groups at $p < 0.05$. Animals were s.c. inoculated in the flank with 1×10^6 cells mixed with matrigel. Mice were housed in groups of 6 and randomly assigned to treatments. Antimicrobial Amx was administered at a concentration of 100 mg/kg in drinking water twice a week. Weight and tumor growth (measured with a caliper and using the formula [length x width x high (mm)]/2 were followed weekly. When tumors reached a size >100 mm^3, mice were randomized into different groups and treated with vehicle (PBS) or Amx in PBS. At the end of treatment, mice were sacrificed, tumors were harvested and measured for size.

2.18. Computation of survival rate in cohorts of TNBC patients

To analyze correlation of OXPHOS gene expression and survivability, Kaplan–Meier survival plots for patients (n = 5143) with TNBC (all grades) with low and high expression of core OXPHOS genes with chemotherapeutic treatments. OXPHOS genes were taken from Human MitoCarta3.0 (https://personal.broadinstitute.org/scalvo/MitoCarta3.0/human.mitocarta3.0.html), ordered by strength of mitochondrial evidence [39]. Multivariate analysis of breast cancer patients from 2010 to 2021 databases, including E-MTAB, E-TABM, and GSE, was performed. All samples and all genes measured with the GPL96 platform and reaching a correlation with survival with a p-value below 0.05 (highlighted in green) or above (highlighted in red) are provided in supplementary file. Filtering was done for untreated (n = 1030) or chemotherapeutically treated (n = 2342) patients. Endocrine therapy treated patients and biased and outlier arrays were excluded. The hazard ratio with 95 % confidence intervals and log-rank p-value as output were determined. The generated p value did not include correction for multiple hypothesis testing by default. Analyses of survivability correlation to OXPHOS gene expression was restricted to the genes shown statistical significance.

2.19. Statistical analysis

All experiments were performed independently at least three times with 2 or 3 replicas. Unless otherwise stated, 2-way ANOVA (multiple comparisons) was applied utilizing the GraphPad Prism software 8.01 0. $P < 0.05$ was considered as significant.

3. Results

3.1. Elevated mitochondrial OXPHOS inversely correlates with poor survival of TNBC patients and is observed in chemoresistant tumors and cells

Recent evidence suggests the presence of OXPHOS-associated tumors associated with poor prognosis after chemotherapy [40,41]. Analysis of data from several thousand TNBC patients shows that survival rate after chemotherapy is reversibly correlated with the expression level of major OXPHOS genes (Fig. 1A, Supplementary Fig. 1). To see if OXPHOS levels correlate with tumor resistance, we analyzed tumor samples from TNBC patients resistant and sensitive to standard chemotherapy. Protein profiling (Fig. 1B–Supplementary file 2) shows a statistically significant increase in OXPHOS protein expression in patients with chemoresistant forms of TNBC tumors (Fig. 1C). To better explore the mechanisms linking chemoresistance and OXPHOS we generated several TNBC cell models, MDA-MB-231 and MDA-MB-468, resistant to the commonly used anticancer drugs cisplatin and cyclophosphamide, respectively. Chemoresistant TNBC cells in MTT assay show significantly higher IC50 values to cisplatin and cyclophosphamide drugs compared to sensitive counterparts (Fig. 1D and E). Protein profiling of the corresponding samples confirmed the increased expression of OXPHOS proteins in chemoresistant cells relative to chemosensitive cells (Fig. 1F and G, Supplementary file 2).

3.2. TNBC chemoresistant cells exhibit enhanced mitochondrial functions

To further investigate the role of mitochondria and mitochondrial OXPHOS in these cell types, we analyzed the basic functions of the organelles. We measured cellular respiration using an oxygraph with a Clark electrode and found a significant increase in oxygen consumption rate (OCR) in chemoresistant cells relative to chemosensitive cells (Fig. 2A–E). This difference was increased when ADP was injected to the camera to promote OXPHOS (Fig. 2A–E, Supplementary file 3). In parallel, we used hormone receptor-positive (ER+/PR+) breast cancer cell line MCF7 as well as healthy (non-cancerous) DF fibroblasts. We found that DF, unlike MCF7, also significantly utilize OXPHOS for cellular respiration (Supplementary file 11). We then determined $\Delta\Psi m$ using the lipophilic cationic dye JC-1 and found that chemoresistant cells have an increased $\Delta\Psi m$ as compared to sensitive counterpart (Supplementary file 4). A parallel mitoGreen staining assay showed an increase in mitochondrial mass (Fig. 2B–F). This was also accompanied by a significant increase in mitochondrial complex II activity (Fig. 2C–G), as well as an increase in ATP synthesis in chemoresistant TNBC cells (Fig. 2D–H). Importantly, these increases were not associated with an increase in mitochondrial mass because samples were normalized for total protein concentration before measurements. The activity of mitochondrial complexes I-IV remained similar in both cell types (Supplementary file 4). Taken together, our data suggest that chemoresistant TNBC cells are predisposed to OXPHOS and exhibit enhanced mitochondrial functions.

3.3. OXPHOS inhibitors as a means to combat TNBC chemoresistance

Our and other recent work has shown that OXPHOS inhibitors can

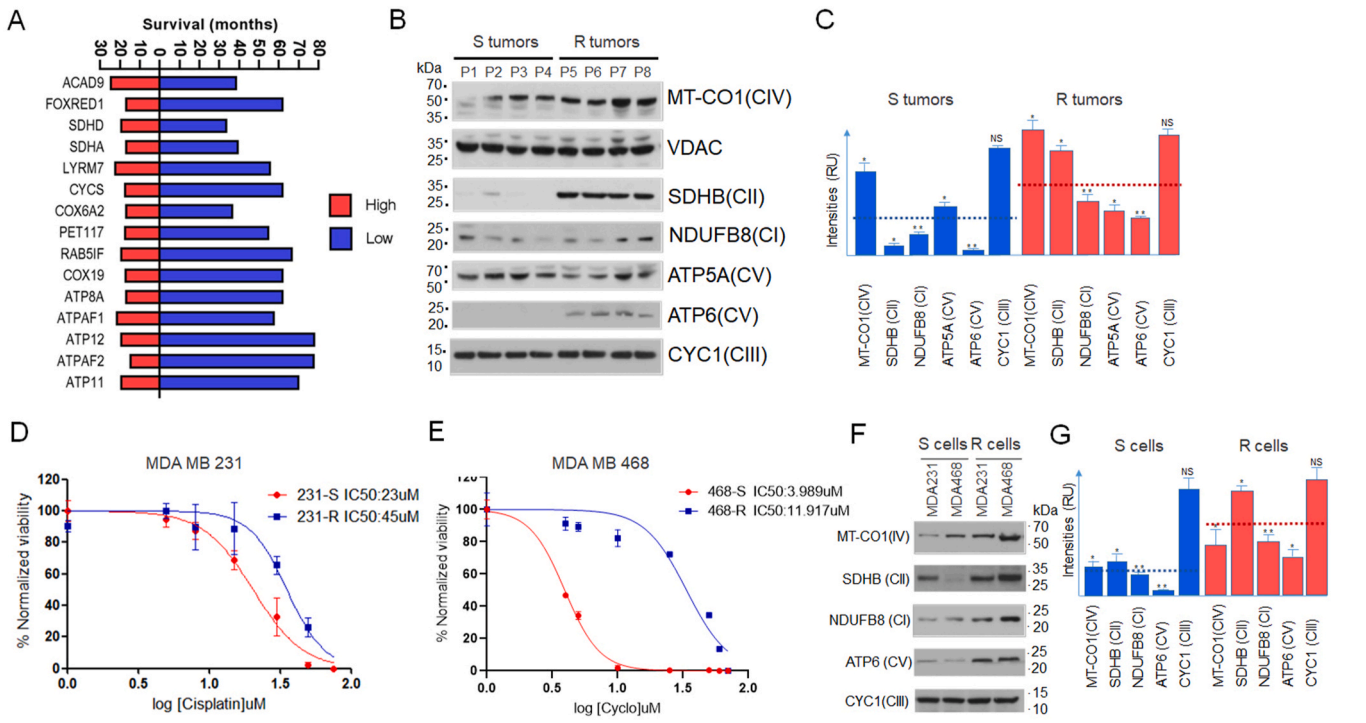

Fig. 1. OXPHOS gene and protein expression levels increase after chemotherapy in TNBC patients and also in chemoresistant cells. (A) High expression of major OXPHOS genes in a cohort of TNBC patients (n = 2342) treated with chemotherapy shows an inverse correlation of OXPHOS gene expression with five-year survival. The Kaplan-Meier data for other OXPHOS genes also show an inverse correlation but are not statistically significant (Supplementary Fig. 1). (B) Protein profiling of major mitochondrial OXPHOS markers by Western blotting from chemoresistant (R) and chemosensitive (S) tumors of TNBC patients and (C) analysis of the corresponding expression signals. Medians are shown as dotted lines ($p < 0.05$ for all matched S and R groups). (D,E) Cell survivability assay for TNBC chemoresistant and sensitive cells. All results are representative of at least three independent experiments with at least three replicas per treatment point. The exact IC50 values are provided for each graph. Data indicate the mean ± SEM. (F) Corresponding protein profiling of major mitochondrial OXPHOS proteins by Western blotting from chemoresistant (R) and chemosensitive (S) TNBC cells and (G) analysis of the corresponding expression signals. Medians are shown as dotted lines ($p < 0.05$ for all matched S and R groups). Loading was normalized by mitochondrial VDAC protein.

target several different malignancies and cancer cell models [42–44]. To identify compounds that preferentially target cancer chemoresistance, TNBC cells were screened using a short list of inhibitors, mostly representing antimicrobials against Gram-negative bacteria because they resemble eukaryotic mitochondria. To identify compounds that preferentially target cancer chemoresistance, we screened a library of antimicrobial compounds, focusing only on drugs against Gram-negative bacteria, as these are the ones that most closely resemble eukaryotic mitochondria (Fig. 3A). The selected compounds were assayed over TNBC cells for attenuating mitochondrial functions of chemoresistant cells with respect to sensitive cells. The idea was to select drugs that would inhibit the metabolic activity of chemoresistant TNBC cells but at the same time would not be toxic to non-cancerous cells even at high doses. Our experiments resulted in two antibiotics, AMX (Amoxicillin sodium), FSS (Fosmidomycin sodium salt), that were active to selected models of resistant TNBC cells (Fig. 3B–E). Since the metabolic (MTT) assay we used, based on the color change of the formazan salt in active mitochondria could affect the accuracy of the measurement, we performed a series of assays with parallel measurement of live cells and showed that both assays may be suitable for this screening (Supplementary file 12). We also showed that the two selected drugs had less effect on MCF7 and no effect at all on normal DF cells (Fig. F,G), implying a specific effect of the drugs on chemoresistant TNBC cells. To investigate in detail the role of the selected OXPHOS inhibitors on the tumorigenic properties of cancer cells, we performed cell adhesion and cell migration (wound healing) assay and showed that both AMX and FSS specifically increase adhesion and decrease migration properties of chemoresistant TNBC cells (Fig. H,I,K,L, Supplementary files 13A,B). As expected neither drugs were able to influence adhesion of MCF7 or normal DF cells (Supplementary file 11). In parallel, we performed colony formation assay and showed that selected drugs reduced the tumorigenic abilities of chemoresistant TNBC cells (Fig. 3J–M).

Before transferring *in vitro* experiments to animal models, we tested their ability to induce MDF. For this purpose, we first measured key mitochondrial parameters by performing the Seahorse experiment. Our results showed that both basal and maximal respiration were presumably decreased in chemoresistant TNBC cell lines after AMX or FSS treatment (Fig. 4A and B, Supplementary file 6). This was in parallel with statistically significant decrease of mitochondrial complex II activities (Fig. 4C and D), ΔΨm (Supplementary file 6), and ATP levels (Fig. 4E and F) in chemoresistant cells. In either MCF7 or normal DF cells these compounds did not significantly suppress OXPHOS (Supplementary file 11). These results suggest that selected inhibitors specifically induce MDF in chemoresistant TNBC cells by suppressing OXPHOS.

3.4. *The OXPHOS inhibitor preferentially reduced the growth of tumors derived from chemoresistant TNBC cells*

We xenoinjected immunocompromised mice with chemoresistant or chemosensitive TNBC cells (1×10^6 cells into each flank) and allowed tumors to grow for 14 days, after which the animals were randomized and assigned to groups. AMX in PBS or PBS alone (control) was orally administered to mice for 7 weeks, and tumor volumes were measured each week (Supplementary Fig. 7). Our results strongly suggested that the OXPHOS inhibitor AMX significantly reduced the growth rate of tumors derived from chemoresistant TNBC cells (Fig. 5B and C).

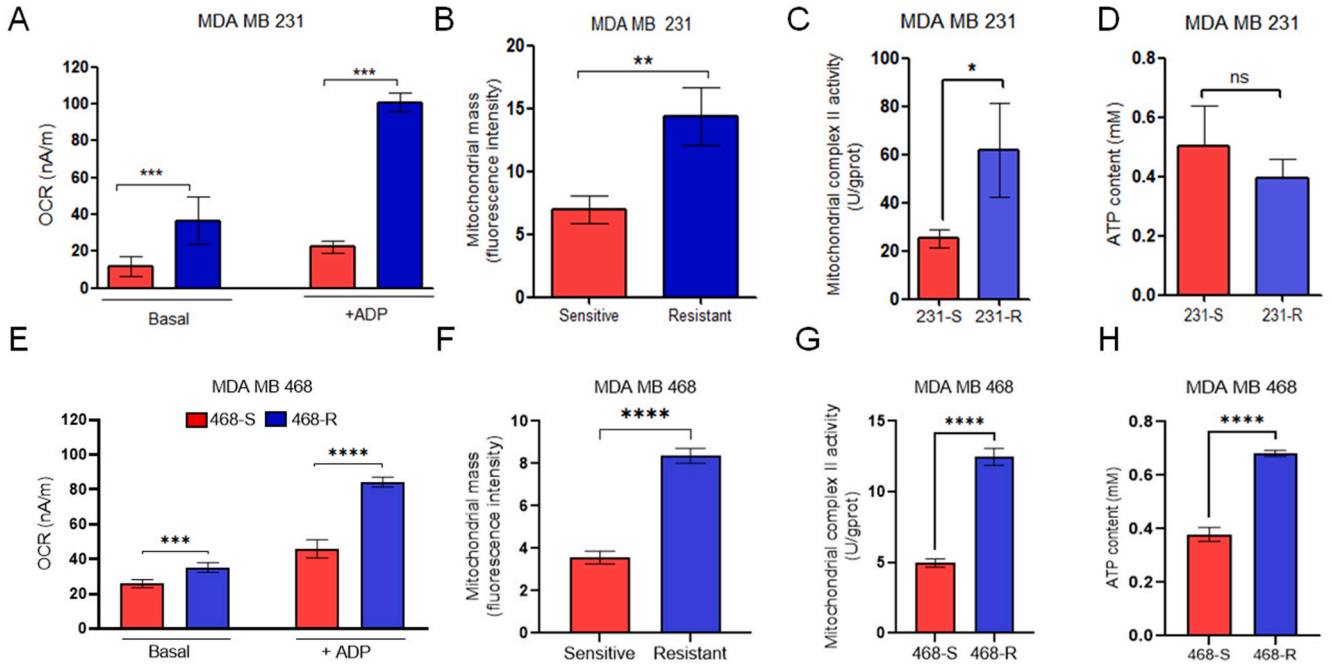

Fig. 2. Chemoresistant cancer cells have more pronounced mitochondrial functions and are predisposed to OXPHOS. (A) Mitochondrial membrane potential (ΔΨm) was measured by incubating cells with cationic dye JC-1. The graph shows the intensity ratios of red (unaggregated) and green (aggregated) signals from mitochondrial reticulum (n = 4). (B) The relative mitochondrial mass ratio was measured by comparing the intensities of cells stained with MitoGreen Tracker and then normalizing the signal intensities to the total number of corresponding cells (n = 4). (C) Cellular oxygen uptake followed by addition of ADP to stimulate OXPHOS (D) was measured using an oxygraph system (Hansatech Instruments Ltd., UK, 2023). (E) Mitochondrial complex II activity and (F) ATP levels were measured spectrofluorimetrically using the appropriate kit and cell number normalization. Experiments were performed independently over three times with three replicas. Values are reported as means ± SD (n ≥ 3). *P < 0.05 compared with the control group.

3.5. The mechanism of targeting TNBC chemoresistance by OXPHOS inhibitor includes reduction of metalloproteinase activity, induction of oxidative stress and mitophagy

We next sought to explore several possible mechanisms for the effects of the OXPHOS inhibitorы on resistant cancer cells. Based on colony growth data, we hypothesized that the characteristic difference between chemoresistant and sensitive TNBC cell phenotypes might be the transition from epithelium to mesenchyme (EMT) [45]. Since one of the main characteristics of the TEM- MET balance is increased matrix metalloproteases (MMPs) activity, we performed zymogram analysis and showed that (i) chemoresistant TNBC cells secrete more active MMPs than their corresponding sensitive counterparts and that (ii) selected OXPHOS inhibitors are able to suppress this activity (Fig. 6A,B,D,E Supplementary file 8). Often, the metastatic potential of cells can be determined by the formation of 3D spheroids emulating cancer stem cells. In this case, we reproduced the ability of TNBC to form mammospheres and showed that in the case of resistant cells their number increases significantly. By exposing the cell medium to AMX or FSS we showed that both drugs reduced the formation of spheroids, much more strongly in chemoresistant cells (Fig. 6C–F). We then examined the role of oxidative stress as one of the possible factors why antimicrobials can specifically kill chemoresistant cancer cells prone to OXPHOS. We measured the accumulation of mitochondrial and intracellular ROS and verified that the selected compounds induced an increase in ROS in both cell lines, and importantly, the increase in ROS was much more pronounced in chemoresistant cells, with high levels of OXPHOS (Fig. 6G and H). In addition, we have shown in vivo that IC50 AMX or FSS-treated aquatic crustaceans *A. salina* also exhibit mitochondrial oxidative stress, which has no effect on eukaryotic viability (Fig. 6I) and confirms the tolerance of the selected drugs to non-cancerous cells. Since ROS can trigger autophagy as a mechanism to remove damaged non-functional parts of the cell [46], we tested this assumption and found that the aforementioned OXPHOS inhibitors indeed induce autophagic events, as evidenced by the accumulation of the lipidated form of LC3A-II (Fig. 6J–Supplementary file 2). We also found that PINK1 and Parkin associated with selective autophagy are partially upregulated following drug treatment of cells in TNBC (Fig. 6J), but not in healthy (DF) cells (Supplementary file 14). Because mitochondria are not only the organelles that produce and control 90 % of ROS in the cell, but also a major target for ROS, we also performed an electron microscope morphologic study of the cells by TEM. Our results show that OXPHOS inhibitor AMX induced mitochondria associated autophagic events (Fig. 6K–Supplementary file 9). Thus, we can conclude that one of the mechanisms of tumor growth suppression in chemoresistant cancer cells may be the reduction of MMP activity and mitophagy induced by oxidative stress.

3.6. Chemoresistance of TNBC cells is reduced by blocking OXPHOS

Since our in vivo results showed that OXPHOS inhibition preferentially suppresses the growth of tumors arising from their chemoresistant OXPHOS-dependent TNBC cells, our final step was to explore the possibility of combinatorial chemotherapeutic targeting cancer resistance by inhibiting OXPHOS with the possibility of re-sensitizing the latter. We tried different combinations of compounds (Supplementary file 10) and found an optimal pharmacological window for AMX, FSS and the anticancer drugs cyclophosphamide and cisplatin for MDA MB 468 (Fig. 7A) and MDA MB 231 (Fig. 7B) TNBC cells. Overall, our results suggest resensitization of chemoresistant TNBC cells by OXPHOS inhibitors.

4. Discussion

Last year marks the 100th anniversary of Otto Warburg's publication of a paper on the dependence of certain malignancies on glycolytic metabolism. This and several subsequent publications have led

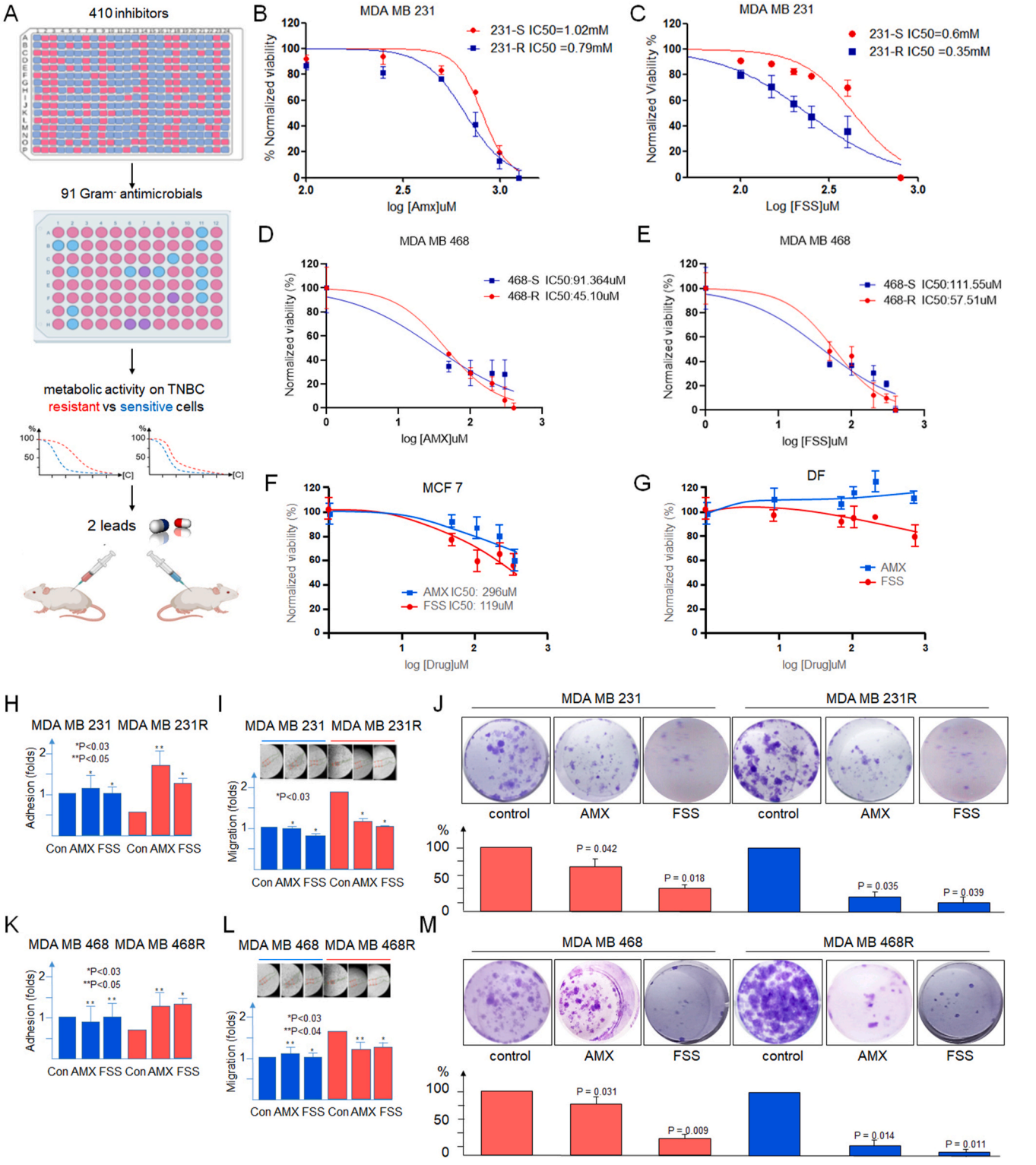

Fig. 3. Specific antimicrobials inhibit the growth of chemoresistant TNBC cells by inducing mitochondrial dysfunction. (A) Screening strategies of antimicrobial libraries. Drugs were first selected based on Gram-negative antimicrobials followed by metabolic assays. The results of identified two drugs that discriminate the growth of chemoresistant and sensitive TNBC cells. (B–E) MTT assay shows a preferential effect on OXPHOS-dependent chemoresistant cancer cells. (F,G) Non-TNBC (MCF7) and non-cancerous cells (DF) were tested in MTT assay against selected drugs. (H,K) Effects of two selected drugs on cell adhesion assay (n = 3x 3 replicas). (I,L) Effects of two selected drugs on cell migration (wound healing) assay (n = 3x 3 replicas). Representative images are shown on top raw. (J,M) Effects of two selected drugs on cancer cell colony growth over three weeks (n = 4). The top row shows examples of stained colonies. Those with greater than 30 cells were counted. Concentration of AMX and FSS used were 200uM and 150uM, respectively. All values are reported as means ± SD (n ≥ 3) compared with the corresponding control groups. The rest of the data are presented in Supplementary Figs. 6 and 11.

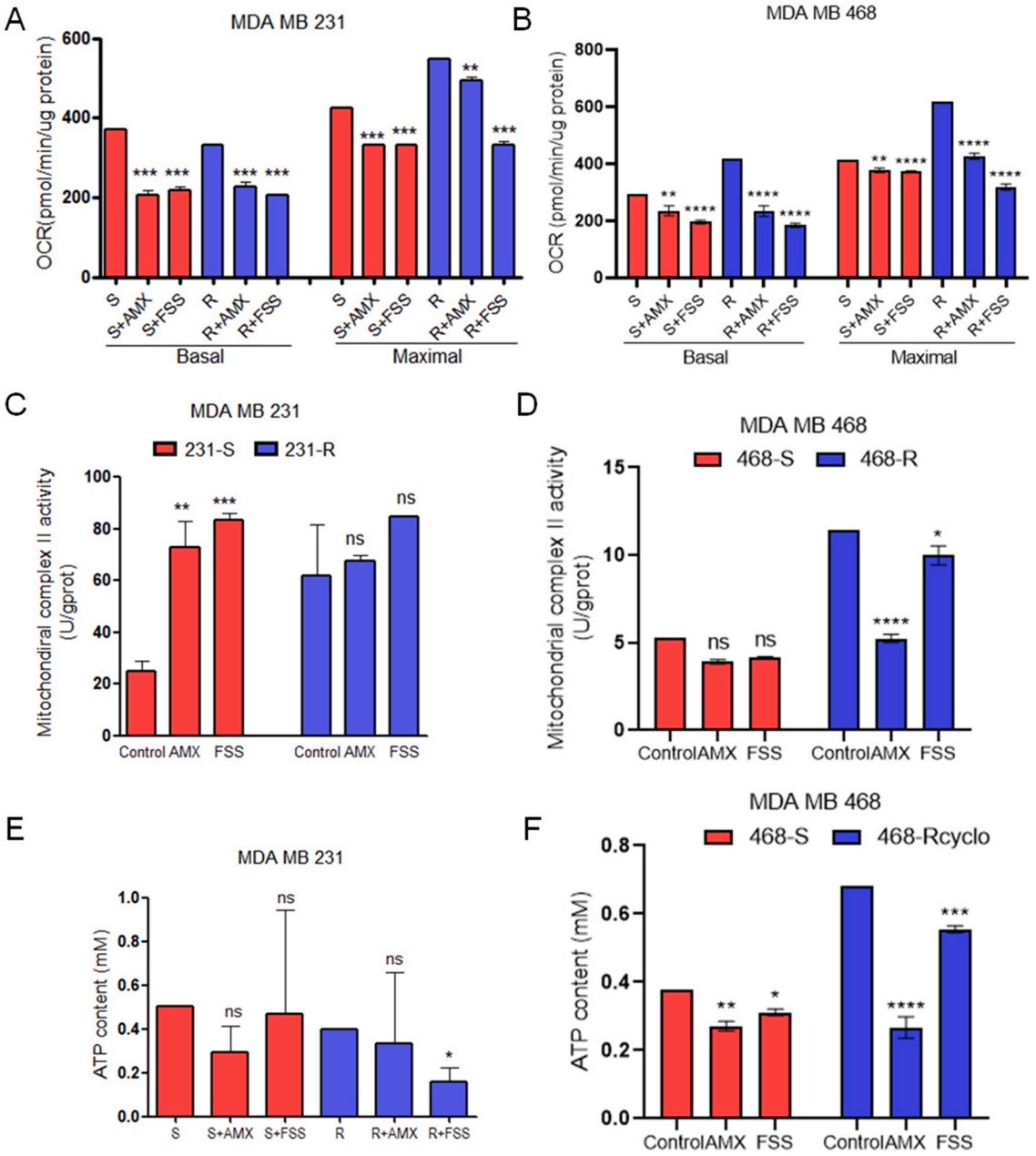

Fig. 4. Specific antimicrobials induce mitochondrial dysfunction by decreasing OXPHOS in chemoresistant TNBC cells. Cellular oxygen uptake and maximal respiration were measured measured using Seahorse XFe-24 analyzer (Agilent Technologies Spain, S.L.) for MDA MB 231 (A) and MDA MB 468 cells untreated or treated with AMX (200μM), FSS (150μM) inhibitors. (C,D) Mitochondrial complex II activity and (E,F) ATP levels were measured spectrofluorimetrically using the appropriate kit and cell number normalization. Experiments were performed independently over three times. Values are reported as means ± SD ($n \geq 3$). *P < 0.02, **P < 0.03, ***P < 0.02, ****P < 0.01 compared with the corresponding control groups. The rest of the data are presented in Supplementary Figs. 4 and 5.

researchers to wonder how rapidly dividing tumor cells, which require more energy, switch from OXPHOS to glycolysis, while mitochondria-mediated OXPHOS provides an order of magnitude more energy [47,48]. In particular, several papers have explained this metabolic paradox by the different bioenergetic kinetics [49]. Thus, rapidly dividing cancer cells prefer a "hit and run" strategy - taking a little at a time but quickly, rather than a "wait and gain" strategy - waiting longer and gaining more ATP. Until recently, this popular narrative helped (but did not replace) the explanation of the Warburg effect.

Our and other works have allowed us to propose a model where glycolysis and OXPHOS exist in parallel in the same heterogeneous malignant tumors [10]. In particular, some cancer cell clones prefer to obtain energy through glycolysis and it is this cell population that has an increased sensitivity to therapeutic intervention. On the other hand, slow dividing cancer clones prefer to proliferate through the OXPHOS pathway, making them more resistant to chemotherapy and radiotherapy. Moreover, such therapy preferentially selects OXPHOS-resistant clones, making the tumor not only to be more aggressive but also metastatically-pronated. For this reason, OXPHOS suppression may serve as one of the new tools to suppress cancer resistance [50].

This is evidenced by our recent review showing decreased survival in cancer patients with breast, gastric, colon, ovarian cancers as well as leukemia and myeloma when OXPHOS genes are overexpressed [11,12,14,16–25] As our study shows, TNBC is no exception, and a number of OXPHOS proteins are preferentially expressed in patients with resistant forms of TNBC and appear to contribute to their survival. This finding provides a rationale to suggest a regimen for the treatment of resistant

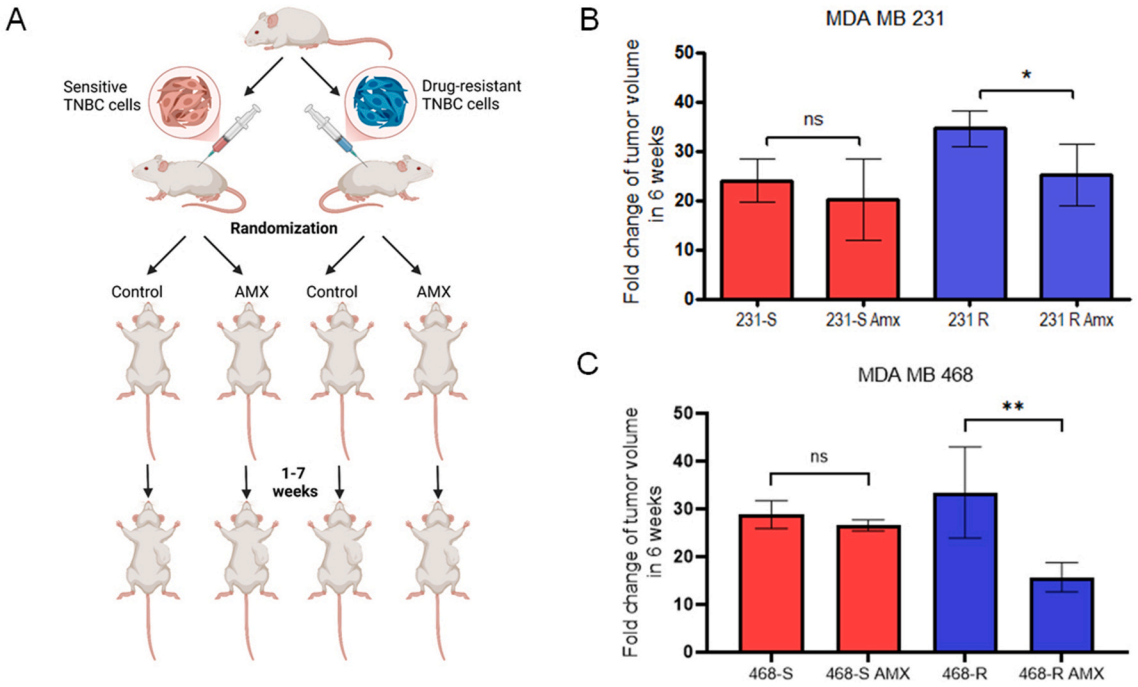

Fig. 5. OXPHOS inhibitor causes significant suppression of tumors arising from TNBC resistant cells. (A) Workflow shows experimental design. Chemosensitive and chemoresistant cells (1×10^6) mixed with matrigel (1:1) were injected into each flank of NMRI-nu mice. When tumors reached a size >100 mm, mice were randomized into different groups of 6 individuals. Mice were given the antimicrobial drug AMX (OXPHOS inhibitor) at a concentration of 100 mg/kg or PBS (control group) in drinking water twice weekly. Tumor weight and growth were monitored weekly (measured with a caliper using the formula [length x width x height (mm)]/2). The diagram shows the results of tumor volumes in mice after 6 weeks in AMX and control groups of (B) MDA MB 231 and (B) MDA MB 468 cells. *P = 0.02, **P = 0.009. The rest of the data are presented in Supplementary file 7.

forms of TNBC when there are elevated OXPHOS levels and conventional therapeutic methods are not effective. It is proposed to repurpose antibactericidal drugs as OXPHOS suppressants, suggesting to affect mitochondria of eukaryotes as precursors of alpha-proteobacteria. This idea, sounded in Kalghatti et al.'s work [51] and more formalized in numerous studies by Michael Lisanti's group, focused mainly on targeting a small population of CSC considered to be the driver of metastatic disease [52,53]. Somewhat later, work by Gotlib's group with AML and our breast cancer group showed proof of principle that a number of antimicrobials can inhibit tumor growth and malignant cancer cells in vivo [35,44,54]. In the current work, we undertook a more massive drug screening focusing on a list of antibiotics against Gram-negative bacteria as their structure mirrors human mitochondria. We showed that inhibition of OXPHOS specifically in resistant cancer cells affects growth suppression of the corresponding tumors in mouse models, while sensitive cancer cells and corresponding tumor models did not show the same response.

In parallel, we tried to find possible mechanisms involved in the inhibition of resistant cancer cells. First, we showed that suppression of OXPHOS by appropriate inhibitors is accompanied by oxidative stress, both intracellular and mitochondrial. Such stress is manifested to a much greater extent in resistant TNBC cells than in sensitive ones, which is most likely due to the fact that in the former the maximal capacity of OCR is almost reached and the enzymes inhibiting ROS as a by-product of mitochondrial electron transfer chain cannot restrain additional stresses. At the same time, sensitive cancer cells still have a buffer zone capable of increasing oxidative ROS load. Since oxidative stress is accompanied by an increase in MDF [55], we identified autophagy activation among some of the possible consequences. We hypothesize that ROS trigger selective autophagy in the form of mitophagy, which should restrain MDF and ultimately interfere with therapeutic intervention. For this reason, the concomitant use of OXPHOS inhibitors with mitophagy inhibitors should serve as a follow-up study phase [33]. Combinatorial exposure of antimicrobials with conventional chemotherapy may serve as an alternative. In this work we have demonstrated this possibility by showing that the combined exposure of small doses of a selected antibiotic with cyclophosphamide on resistant cancer cells multiplies the ICs of the latter. Thus, exposure to antimicrobial agents reopens the pharmacologic window for chemotherapy, allowing a significant reduction in the cytotoxic effects of chemotherapeutic agents on normal cells.

In addition to the above-mentioned mechanisms, we found suppression of metalloproteinase activity under the influence of bactericidal antibiotics. Metalloproteinases represent one of the ways to overcome cancer cell resistance and subsequent metastasis. Activated through mutations leading to overexpression of cytokines and interleukins, proteinases help cancer cells to escape primary tumors by overcoming cell adhesion and disseminating to distal tissue regions. In the current study we have shown that it is the resistant cancer cells that have greater potential to metastasize (loss of adhesion, increased migration) and it is these properties that are inhibited by selected OXPHOS inhibitors. This fact offers another possibility of combinatorial targeted intervention against resistant cancer cells.

It is also an open question what other OXPHOS inhibitors among antimicrobials can be used to suppress chemoresistant tumors and what approaches can be taken to improve their delivery. In particular, in screening the library, we found several other drugs with the ability to inhibit OXPHOS-dependent resistant cells. First, it should be considered that many of the short listed inhibitors have only been tested in veterinary medicine, not in humans, and ethically should not be proposed for use without appropriate phase testing, which would make their potential use more expensive. Secondly, an alternative approach could be to reduce the overall cytotoxicity of the drug by appropriate chemical modification and attachment of a triphenylphosphonium group, TPP [35]. This approach has advantages, but the TPP group itself can severely depolarize mitochondria and thereby reduce the efficiency of targeted drug delivery. In any outcome, this will require an additional series of animal trials. Despite the above observations on the significant

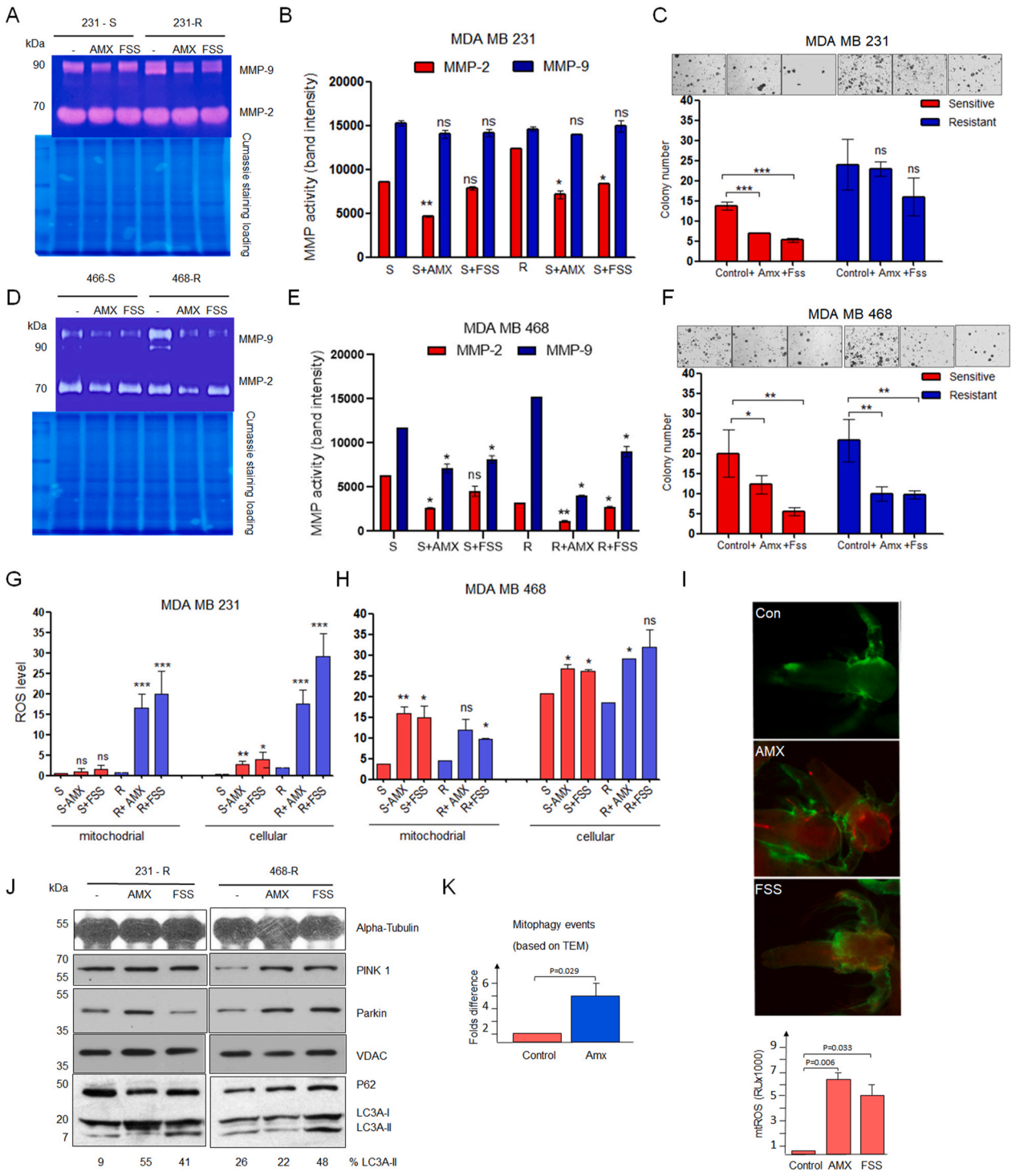

Fig. 6. OXPHOS inhibitor causes the reduction of MMP activity and oxidative stress-associated mitophagy. (A,D) Zymogram assay showing increased MMP activity in chemoresistant *vs.* chemosensitive supernatants of TNBC cells after AMX (750μM) or FSS (350μM) treatment, and (B,E) corresponding measurement of signal intensities. Normalization of probes was done by overall protein concentrations and Cumassie staining loading controls. (C,F) Effect of selected antimicrobials on the 3D-tumospher formation of TNBC-sensitive and chemoresistant cells grown as second generation under non-adherent conditions for 6 days in the absence or presence of (200μM), FSS (150μM), to form spheroids. Representative images of treated cells show a decrease in spheroid number. The results are the mean of 5 independent experiments. The data indicate the mean ± SEM. The p-values, all relative to controls, were statistically significant (*$p < 0.05$,**$p < 0.03$,***$p < 0.02$). (G,H left) Mitochondrial and (G,H right) intracellular ROS accumulation was measured with MitoSoxRed and H2DCF-DA reagents, respectively ($n = 4$). The data indicate the mean ± SEM. The p-values, all relative to controls, were statistically significant (all $p < 0.05$). (I) In vivo oxidative stress was measured in A.salina nauplii by incubating 500 species per well with AMX (700μM), FSS(350μM), or PBS (control) followed by adding MitoSoxRed and MitoGreen. mtROS measurements are shown below after normalization to overall green intensities. (J) Results of Western blot for the autophagy (LC3AII and p62) and mitophagy (PINK1, Parkin) markers. On the bottom is shown measurements (%) of autophagy induction by the ratio of LC3AII (lipidated) vs LC3AI (nonlipidated) forms. (F) Measurements of mitophagic events in MDA MB 231 R cells treated or untreated with Amx for 3 days. Results are based on $n = 6$ TEM images (Supplementary Fig. 9).

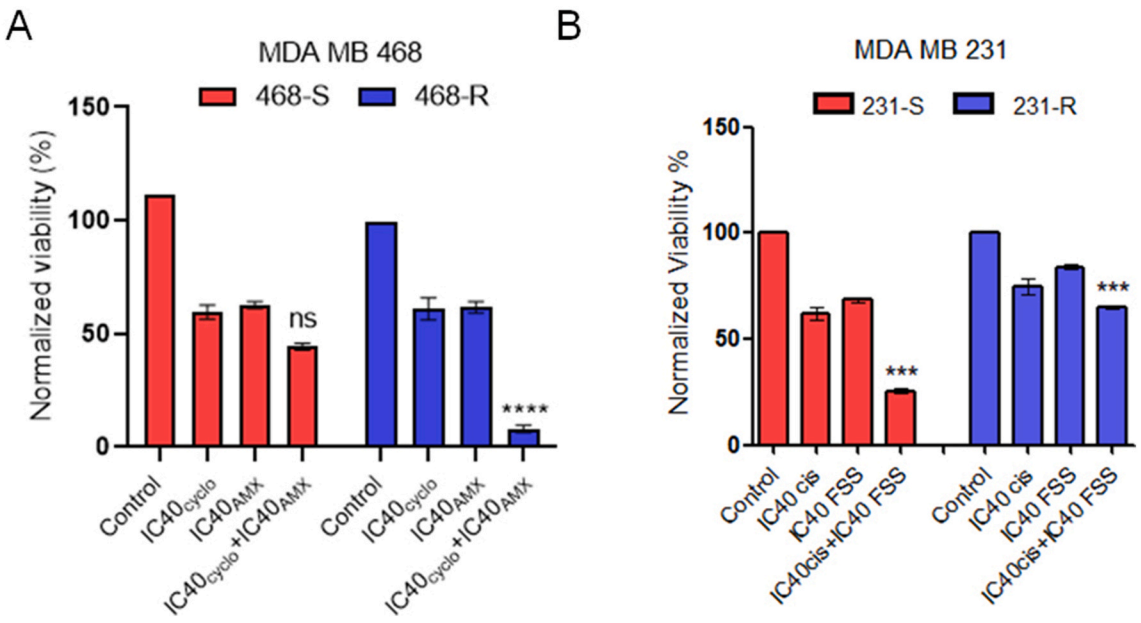

Fig. 7. Combinatorial treatment of OXPHOS inhibitor and chemotherapeutic drugs. (A) Workflow demonstrating combination of OXPHOS inhibitor and chemotherapeutic agent (cyclophosphamide) on chemoresistant and sensitive TNBC cells (B) Cells were treated with increasing concentrations of OXPHOS inhibitor AMX in combination with low doses of cyclophosphamide, followed by survivability assay, and the half-maximal inhibitory concentrations (IC50) were calculated. Results are the mean of three independent experiments (n = 5). Data indicate the mean ± SEM (all *P < 0.05). The rest of the data are presented in Supplementary file 10.

role of OXPHOS in malignancy resistance, we should not exclude other factors. In particular, ATP-dependent transporters [56], EMT [57], abnormal neovascularization in the tumor microenvironment, alterations in antigen presentation pathways [58], as well as multiple lines of evidence linking tumor resistance and enhanced DNA damage response, particularly for cancer stem cells [59] point to an unexplored part of the iceberg, but that is beyond the scope of this paper.

In conclusion, based on current and previous data, our working hypothesis suggests that OXPHOS is more characteristic of a small population of resistant cancer cells (contradicts the Warburg effect), while the bulk of rapidly dividing cells are associated with glycolysis (supports the Warburg effect). Moreover, anticancer chemotherapy or radiotherapy promotes tumor evolution and selects cells with functional mitochondria in the OXPHOS mode from the total mass of malignant tumor [60]. In contrast, rapidly dividing glycolytic cells are suppressed by therapeutic interventions. We do not know whether OXPHOS-prone cells possess a spectrum of mutations that create chemoresistance or whether they simply possess a stemness property that allows them to dissociate and specifically differentiate into distant organs, but this question appears to be closely related to cell bioenergetics [61]. These and other such questions need to be clarified, as they are extremely important not only for the sake of scientific curiosity, but also for the more pragmatic goals of personalized medicine.

CRediT authorship contribution statement

Cemile Uslu: Data curation, Formal analysis, Investigation, Methodology, Software, Validation, Visualization. **Eda Kapan:** Data curation, Formal analysis, Investigation, Methodology, Software, Validation. **Alex Lyakhovich:** Conceptualization, Data curation, Formal analysis, Funding acquisition, Investigation, Methodology, Project administration, Resources, Software, Supervision, Validation, Visualization, Writing – original draft, Writing – review & editing.

Data availability

Data will be made available on request.

Funding

A.L. and lab members were supported by the TUBITAK 2232A program, an international fellowship for outstanding researchers (Project 121C096) and TUBITAK 1001 grant (Project 124Z377).

Declaration of competing interest

The authors declare the following financial interests/personal relationships which may be considered as potential competing interests: One of the co-authors of this article, Cemile Uslu, is the recipient of the AACR scholar award. In accordance with AACR guidelines, we may embargo publication of this manuscript until April 25, 2025, the start of the AACR annual meeting. If there are other authors, they declare that they have no known competing financial interests or personal relationships that could have appeared to influence the work reported in this paper.

Acknowledgments

We thank Tumor Bank of Vall d'Hebron University Hospital Biobank for providing TNBT samples. We are also grateful to Prof. Ales Hampl for providing the transmission electron microscopy facilities.

Appendix A. Supplementary data

Supplementary data to this article can be found online at https://doi.org/10.1016/j.redox.2025.103637.

References

[1] Global cancer observatory. https://gco.iarc.fr/en. (Accessed 22 December 2024).
[2] Information and Resources about cancer: breast, colon, lung, prostate, skin | American cancer society. https://www.cancer.org/..html. (Accessed 23 December 2024).
[3] G. Bianchini, J.M. Balko, I.A. Mayer, M.E. Sanders, L. Gianni, Triple-negative breast cancer: challenges and opportunities of a heterogeneous disease, Nat. Rev. Clin. Oncol. 13 (11) (2016) 674–690, https://doi.org/10.1038/nrclinonc.2016.66.

[4] Edgardo Rivera, Henry Gomez, Chemotherapy resistance in metastatic breast cancer - the evolving role of ixabepilone, Breast Cancer Res. 12 (Suppl 2) (2010) 1–12.

[5] E.A. O'Reilly, et al., The fate of chemoresistance in triple negative breast cancer (TNBC), BBA Clin. 3 (2015) 257–275, https://doi.org/10.1016/j.bbacli.2015.03.003.

[6] O. Warburg, F. Wind, E. Negelein, Über den Stoffwechsel von Tumoren im Körper, Klin. Wochenschr. 5 (19) (1926) 829–832, https://doi.org/10.1007/BF01726240.

[7] H.G. Crabtree, Observations on the carbohydrate metabolism of tumours, Biochem. J. 23 (3) (Jan. 1929) 536, https://doi.org/10.1042/BJ0230536.

[8] A.J. Levine, A.M. Puzio-Kuter, The control of the metabolic switch in cancers by oncogenes and tumor suppressor genes, Science 330 (6009) (2010) 1340–1344, https://doi.org/10.1126/science.1193494.

[9] J. Zheng, Energy metabolism of cancer: glycolysis versus oxidative phosphorylation, Oncol. Lett. 4 (6) (2012) 1151–1157, https://doi.org/10.3892/ol.2012.928 (review).

[10] C. Uslu, E. Kapan, A. Lyakhovich, Cancer resistance and metastasis are maintained through oxidative phosphorylation, Cancer Lett. 587 (January) (2024) 216705, https://doi.org/10.1016/j.canlet.2024.216705.

[11] J.T. Hagen, et al., Intrinsic adaptations in OXPHOS power output and reduced tumorigenicity characterize doxorubicin resistant ovarian cancer cells, Biochim. Biophys. Acta Bioenerg. 1863 (8) (Nov. 2022) 148915, https://doi.org/10.1016/J.BBABIO.2022.148915.

[12] S. Dar, et al., Bioenergetic adaptations in chemoresistant ovarian cancer cells, Sci. Rep. 7 (1) (2017) 1–17, https://doi.org/10.1038/s41598-017-09206-0.

[13] K. min Lee, et al., MYC and MCL1 cooperatively promote chemotherapy-resistant breast cancer stem cells via regulation of mitochondrial oxidative phosphorylation, Cell Metab. 26 (4) (2017) 633–647.e7, https://doi.org/10.1016/j.cmet.2017.09.009.

[14] C.Y. Huang, et al., Glucose metabolites exert opposing roles in tumor chemoresistance, Front. Oncol. 9 (39) (2019), https://doi.org/10.3389/fonc.2019.01282.

[15] C. Denise, et al., 5-Fluorouracil resistant colon cancer cells are addicted to OXPHOS to survive and enhance stem-like traits, Oncotarget 6 (39) (Oct. 2015) 41706–41721, https://doi.org/10.18632/ONCOTARGET.5991.

[16] T.T. Vellinga, et al., SIRT1/PGC1a-Dependent increase in oxidative phosphorylation supports chemotherapy resistance of colon cancer, Clin. Cancer Res. 21 (12) (2015) 2870–2879, https://doi.org/10.1158/1078-0432.CCR-14-2290.

[17] A. Cruz-Bermúdez, et al., Cisplatin resistance involves a metabolic reprogramming through ROS and PGC-1α in NSCLC which can be overcome by OXPHOS inhibition, Free Radic. Biol. Med. 135 (March) (2019) 167–181, https://doi.org/10.1016/j.freeradbiomed.2019.03.009.

[18] B.J. Wylie, et al., Oncogene ablation-resistant pancreatic cancer cells depend on mitochondrial function, Nature 514 (7524) (2014) 628–632, https://doi.org/10.1038/nature13611.Oncogene.

[19] R. Masoud, et al., Targeting mitochondrial complex I overcomes chemoresistance in high OXPHOS pancreatic cancer, Cell Reports Med 1 (8) (2020), https://doi.org/10.1016/j.xcrm.2020.100143.

[20] T. Farge, et al., Chemotherapy-resistant human acute myeloid leukemia cells are not enriched for leukemic stem cells but require oxidative metabolism, Cancer Discov. 7 (7) (2017) 716–735, https://doi.org/10.1158/2159-8290.CD-16-0441.

[21] A. Roma, et al., Glutamine metabolism mediates sensitivity to respiratory complex II inhibition in acute myeloid leukemia, Mol. Cancer Res. 20 (11) (Nov. 2022) 1659–1673, https://doi.org/10.1158/1541-7786.MCR-21-1032/708293/AM/GLUTAMINE-METABOLISM-MEDIATES-SENSITIVITY-TO.

[22] R. Guièze, et al., Mitochondrial reprogramming underlies resistance to BCL-2 inhibition in lymphoid malignancies, Cancer Cell 36 (4) (2019) 369–384.e13, https://doi.org/10.1016/j.ccell.2019.08.005.

[23] L. Zhang, et al., Metabolic reprogramming toward oxidative phosphorylation identifies a therapeutic target for mantle cell lymphoma, Sci. Transl. Med. 11 (491) (2019), https://doi.org/10.1126/SCITRANSLMED.AAU1167.

[24] O. Garbarino, et al., PLX4032 resistance of patient-derived melanoma cells: crucial role of oxidative metabolism, Front. Oncol. 13 (July) (2023) 1–20, https://doi.org/10.3389/fonc.2023.1210130.

[25] G. Cheng, et al., Mitochondria-targeted magnolol inhibits OXPHOS, proliferation, and tumor growth via modulation of energetics and autophagy in melanoma cells, Cancer Treat. Res. Commun. 25 (2020) 100210, https://doi.org/10.1016/j.ctarc.2020.100210.

[26] C. Bosc, M.A. Selak, J.E. Sarry, Resistance is futile: targeting mitochondrial energetics and metabolism to overcome drug resistance in cancer treatment, Cell Metab. 26 (5) (2017) 705–707, https://doi.org/10.1016/j.cmet.2017.10.013.

[27] D.F. Boreel, P.N. Span, S. Heskamp, G.J. Adema, J. Bussink, Targeting oxidative phosphorylation to increase the efficacy of radio- and immune-combination therapy, Clin. Cancer Res. 27 (11) (2021) 2970–2978, https://doi.org/10.1158/1078-0432.CCR-20-3913.

[28] R. Lamb, et al., Antibiotics that target mitochondria effectively eradicate cancer stem cells, across multiple tumor types: treating cancer like an infectious disease, Oncotarget 6 (7) (2015) 4569–4584, https://doi.org/10.18632/oncotarget.3174.

[29] M.E. Lleonart, R. Grodzicki, D.M. Graifer, A. Lyakhovich, Mitochondrial dysfunction and potential anticancer therapy, Med. Res. Rev. 37 (6) (2017) 1275–1298, https://doi.org/10.1002/med.21459.

[30] C. Scatena, et al., Doxycycline, an inhibitor of mitochondrial biogenesis, effectively reduces cancer stem cells (CSCs) in early breast cancer patients: a clinical pilot study, Front. Oncol. 8 (OCT) (2018), https://doi.org/10.3389/fonc.2018.00452.

[31] M. Fiorillo, F. Sotgia, M.P. Lisanti, Energetic' cancer stem cells (e-CSCs): a new hyper-metabolic and proliferative tumor cell phenotype, driven by mitochondrial energy, Front. Oncol. 9 (FEB) (2019) 1–15, https://doi.org/10.3389/fonc.2018.00677.

[32] P. Shyamsunder, et al., Impaired mitophagy in Fanconi anemia is dependent on mitochondrial fission, Oncotarget 7 (36) (2016) 58065–58074, https://doi.org/10.18632/oncotarget.11161.

[33] M. Esner, D. Graifer, M.E. Lleonart, A. Lyakhovich, Targeting cancer cells through antibiotics-induced mitochondrial dysfunction requires autophagy inhibition, Cancer Lett. 384 (October) (2017) 60–69, https://doi.org/10.1016/j.canlet.2016.09.023.

[34] U. Kumari, W. Ya Jun, B. Huat Bay, A. Lyakhovich, Evidence of mitochondrial dysfunction and impaired ROS detoxifying machinery in Fanconi Anemia cells, Oncogene 33 (2) (2014) 165–172, https://doi.org/10.1038/onc.2012.583.

[35] J.A. Pavlova, et al., Triphenilphosphonium analogs of chloramphenicol as dual-acting antimicrobial and antiproliferating agents, Antibiotics 10 (5) (2021) 1–22, https://doi.org/10.3390/antibiotics10050489.

[36] A. Epanchintsev, P. Shyamsunder, R.S. Verma, A. Lyakhovich, IL-6, IL-8, MMP-2, MMP-9 are overexpressed in Fanconi anemia cells through a NF-κB/TNF-α dependent mechanism, Mol. Carcinog. 54 (12) (2015) 1686–1699, https://doi.org/10.1002/mc.22240.

[37] E. Abad, L. Civit, D. Potesil, Z. Zdrahal, A. Lyakhovich, Enhanced DNA damage response through RAD50 in triple negative breast cancer resistant and cancer stem-like cells contributes to chemoresistance, FEBS J. 288 (7) (2021) 2184–2202, https://doi.org/10.1111/febs.15588.

[38] H. Fadda, R.H. Khan, Y. Shqair, C. Uslu, A.V. Panov, A. Lyakhovich, Antibacterials exert toxic effects on aquatic organisms by inhibiting respiration, inducing oxidative stress, mitochondrial dysfunction and autophagy, Aquat. Toxicol. 280 (February) (2025) 107284, https://doi.org/10.1016/j.aquatox.2025.107284.

[39] S. Rath, et al., MitoCarta3.0: an updated mitochondrial proteome now with sub-organelle localization and pathway annotations, Nucleic Acids Res. 49 (D1) (Jan. 2021) D1541–D1547, https://doi.org/10.1093/NAR/GKAA1011.

[40] W. Chen, et al., A robust panel based on mitochondrial localized proteins for prognostic prediction of lung adenocarcinoma, Oxid. Med. Cell. Longev. 2021 (2021), https://doi.org/10.1155/2021/7569168.

[41] V. Sica, J.M. Bravo-San Pedro, G. Stoll, G. Kroemer, Oxidative phosphorylation as a potential therapeutic target for cancer therapy, Int. J. Cancer 146 (1) (2020) 10–17, https://doi.org/10.1002/ijc.32616.

[42] D.F. Boreel, et al., 327: inhibition of OXPHOS induces a metabolic switch and reduces hypoxia in immunocompetent tumor models, Radiother. Oncol. 194 (October) (2024) S5194–S5198, https://doi.org/10.1016/s0167-8140(24)00982-4.

[43] T. Rossi, et al., BET inhibitors (BETi) influence oxidative phosphorylation metabolism by affecting mitochondrial dynamics leading to alterations in apoptotic pathways in triple-negative breast cancer (TNBC) cells, Cell Prolif. (January) (2024) 1–14, https://doi.org/10.1111/cpr.13730.

[44] E. Abad, et al., Common metabolic pathways implicated in resistance to chemotherapy point to a key mitochondrial role in breast cancer, Mol. Cell. Proteomics 18 (2) (2019) 231–244, https://doi.org/10.1074/mcp.RA118.001102.

[45] E.M. Grasset, et al., Triple negative breast cancer metastasis involves complex EMT dynamics and requires vimentin HHS Public Access, Sci. Transl. Med. 14 (656) (2022) 7571, https://doi.org/10.1126/scitranslmed.abn7571.Triple.

[46] G. Filomeni, D. De Zio, F. Cecconi, Oxidative stress and autophagy: the clash between damage and metabolic needs, Cell Death Differ. 22 (3) (2015) 377–388, https://doi.org/10.1038/cdd.2014.150.

[47] M.V. Liberti, J.W. Locasale, The Warburg effect: how does it benefit cancer cells? Trends Biochem. Sci. 41 (3) (2016) 211–218, https://doi.org/10.1016/j.tibs.2015.12.001.

[48] K. Vasan, M. Werner, N.S. Chandel, Mitochondrial metabolism as a target for cancer therapy, Cell Metab. 32 (3) (2020) 341–352, https://doi.org/10.1016/j.cmet.2020.06.019.

[49] T. Pfeiffer, S. Schuster, S. Bonhoeffer, Cooperation and competition in the evolution of ATP-producing pathways, Science 292 (5516) (2001) 504–507, https://doi.org/10.1126/science.1058079.

[50] K.W. Evans, et al., Oxidative phosphorylation is a metabolic vulnerability in chemotherapy-resistant triple-negative breast cancer, Cancer Res. 81 (21) (2021) 5572–5581, https://doi.org/10.1158/0008-5472.CAN-20-3242.

[51] S. Kalghatgi, et al., Bactericidal antibiotics induce mitochondrial dysfunction and oxidative damage in mammalian cells, Sci. Transl. Med. 5 (192) (2013), https://doi.org/10.1126/scitranslmed.3006055.

[52] Marco Fiorillo, et al., Bedaquiline, an FDA-approved antibiotic, inhibits mitochondrial function and potently blocks the proliferative expansion of stem-like cancer cells (CSCs), Aging (Albany. NY) 8 (8) (2016) 1593–1607.

[53] B. Ozsvari, et al., Mitoriboscins: mitochondrial-based therapeutics targeting cancer stem cells (CSCs), bacteria and pathogenic yeast, Oncotarget 8 (40) (2017) 67457–67472, https://doi.org/10.18632/oncotarget.19084.

[54] E.M. Kuntz, et al., Targeting mitochondrial oxidative phosphorylation eradicates therapy-resistant chronic myeloid leukemia stem cells, Nat. Med. 23 (10) (2017) 1234–1240, https://doi.org/10.1038/nm.4399.

[55] A. Lyakhovich, D. Graifer, Mitochondria-mediated oxidative stress: old target for new drugs, Curr. Med. Chem. 22 (26) (Sep. 2015) 3040–3053, https://doi.org/10.2174/0929867322666150729114036.

[56] M.M. Gottesman, T. Fojo, S.E. Bates, Multidrug resistance in cancer: role of ATP-dependent transporters, Nat. Rev. Cancer 2 (1) (2002) 48–58, https://doi.org/10.1038/nrc706.

[57] A. Singh, J. Settleman, EMT, cancer stem cells and drug resistance: an emerging axis of evil in the war on cancer, Oncogene 29 (34) (2010) 4741–4751, https://doi.org/10.1038/onc.2010.215.
[58] R. Bai, et al., Mechanisms of cancer resistance to immunotherapy, Front. Oncol. 10 (August) (2020) 1–12, https://doi.org/10.3389/fonc.2020.01290.
[59] E. Abad, D. Graifer, A. Lyakhovich, DNA damage response and resistance of cancer stem cells, Cancer Lett. 474 (December 2019) (2020) 106–117, https://doi.org/10.1016/j.canlet.2020.01.008.
[60] C. Kim, et al., Chemoresistance evolution in triple-negative breast cancer delineated by single-cell sequencing, Cell 173 (4) (2018) 879–893.e13, https://doi.org/10.1016/j.cell.2018.03.041.
[61] I. Karp, A. Lyakhovich, Targeting cancer stem cells with antibiotics inducing mitochondrial dysfunction as an alternative anticancer therapy, Biochem. Pharmacol. 198 (January) (2022) 114966, https://doi.org/10.1016/j.bcp.2022.114966.